Impact of Wind Turbines on Weather Radars

Don Quijote and Sancho Panza after an unsuccessful attack on a windmill, by Gustave Doré.

> *En un lugar de la Mancha, de cuyo nombre no quiero acordarme, no ha mucho tiempo que vivía un hidalgo de los de lanza en astillero, adarga antigua, rocín flaco y galgo corredor.*
> "In a place in La Mancha, whose name I do not want to recall, there dwelt not so long ago a gentleman of the type wont to keep an unused lance, an old shield, a greyhound for racing, and a skinny old horse."

Don Quijote de la Manch (published 1605 and 1615), Miguel de Cervantes Saavedra (1547-1616)

The expressions "tilting at windmills" and "fighting windmills" come from this story.

Table of contends.

This document is marked as a working document of the OPERA II programme, WD_2006_18.

1. Introduction

2. Introduction

On a general basis, blockage of weather radar beam by any obstruction could result in weather radar not being able to perform its nominal purposes, namely to monitor rain (or snow) fall and wind. Even partial, such blockage of the radar beam is nearly as devastating as the weather radars are calibrated in absolute terms of precipitation since it will result in errors in the estimated precipitation.

To this respect, it currently appears that wind mill's turbines are becoming a serious candidate for potential huge impact to weather radar. Indeed, in Europe, many countries are looking for renewable sources of energy, and the numbers of wind turbines are quickly growing.

For example, in Denmark, which is one of the pioneer in this field, about 20 % of the energy consumption today, is delivered by wind turbines. Huge wind mill farms have been established or are planned to be set up in the near future. Figure 1.1 shows part of one of the largest at sea, called Horns Rev Wind Mill Farm, where 80 wind turbines (each generating 2 MW of power) are placed in an area of less than 20 km^2. Fortunately, this particular wind mill farm is situated about 30 nautical miles from the Danish weather radar Rømø but there are cases where the wind mill farms are situated very close to the radar sites and obviously present serious impact on radar products (See example for the Danish weather radar Stevns in figure 8.2)

Figure 1.1: *Horns Rev Wind Mill Farm, Jutland, Denmark*

A theoretical study performed by Meteo France, presented at the OPERA II meeting in Exeter in April 2005, highlighted that the influence of Wind Turbines on the use of weather radars is not only limited to the blockage effect but has, due to high level wind mills Radar Cross Section (RCS) and rotation of the blades, impact on precipitation and Doppler products, results confirmed by recent measurements (see sections 2 and 3).

This study has been validated by the French Radiocommunication Authority (ANFR) in an official Report, that recommends that the placing of wind mills should be avoided at ranges lower than 5 or 10 km (respectively for C and S band radars) and coordinated with the weather radar operators at distances up to 20 km or 30 km (respectively for C and S band radars).

These recommendations have been considered and adopted within the OPERA programme as given in section 9.

3. Theory

The propagation of electromagnetic radiation from an antenna expands spherically and the power density at a long range R from the transmitting antenna is given by

$$P_D = \frac{P_t G_t}{4\pi R^2}$$

where P_t and G_t are transmitted power and antenna gain, respectively. The long distance here is called the far field and the spherical surface of uniform power density appears to be flat. This is where (per definition) the phase differences is less than 1/16 of a wavelength when one neglects the curvature of those spheres of the power densities. The antenna can be modelled as a point.

The shape of the power density in the far field is Gaussian, there will be refraction around possible obstructions, and a there will be a loss from possible obstructions, proportional with the area of the obstruction.

Coming closer to the radar, one enters the near field. The distribution of power in a section across the propagation direction is chaotic, and the antenna can not be modelled as a point. All coverage of the aperture of the antenna in this zone will block as mush of the energy as the blocked area is to the aperture area of the antenna. It is possible to calculate the power flow (Poynting's vector) and the power density in this zone, but it is not trivial [see Kirk T. McDonald, www.hep.princeton.edu/~mcdonald/examples].

Using the above definition of the point where the far field starts, where the phase differences is more than 1/16 of a wavelength, this distance R_{ff} , can be calculated [see EW and RADAR Systems Engineering Handbook]:

$$R_{ff} = 2 \cdot D^2 / \lambda$$

Where D is the antenna aperture and λ is the wavelength. In figure 2.1, this distance is calculated for different type of antennas. In this figure, curve D is calculated for an antenna with parabolic reflector, one which is in common use for weather radars. D can be taken as the diameter of the reflector.

At the point E in figure 2.1, the complexity of the power density starts, and at greater distances than R_{ff}, where Y=1, wee have the far field.

In figure 2.2, a simple model for the zones is shown [from Tage Andersson, SMHI, 1985]. The antennas radiation field is dived into three zones, the ultra near zone, $r < 0.1*R_{ff}$, the near zone, $0.1*R_{ff} < r < R_{ff}$ and the far zone $R_{ff} < r$.

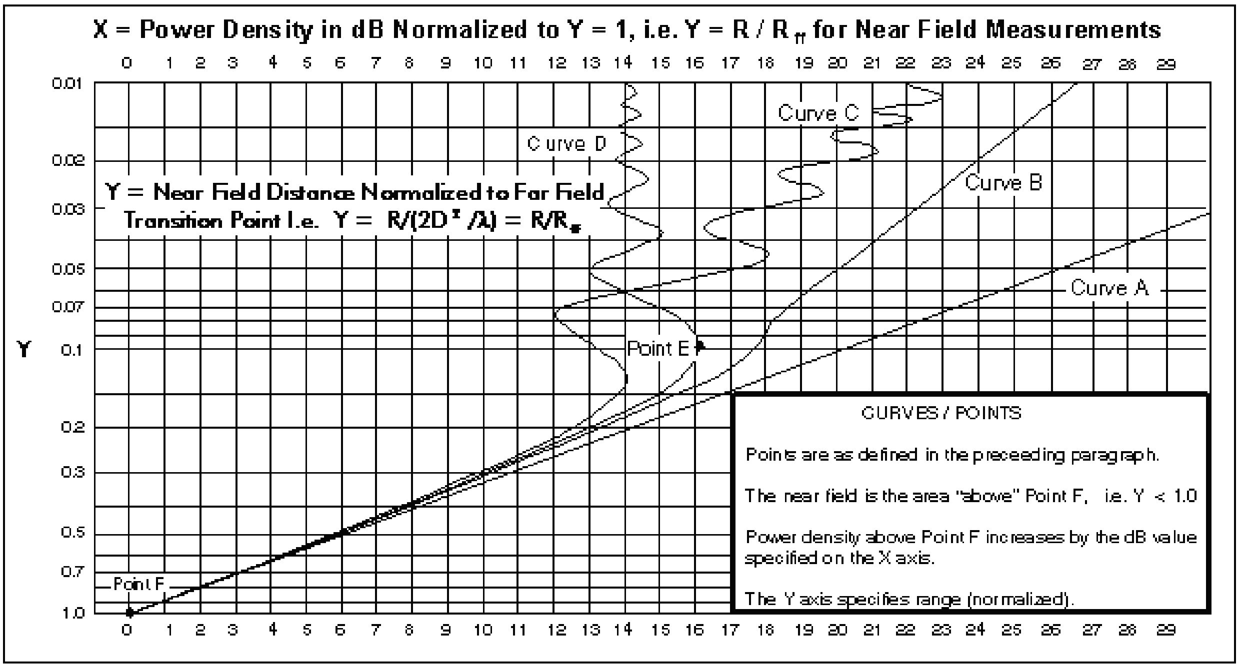

Figur 2.1. *Power density along the antenna axis (from EW and RADAR Systems Engineering Handbook)*

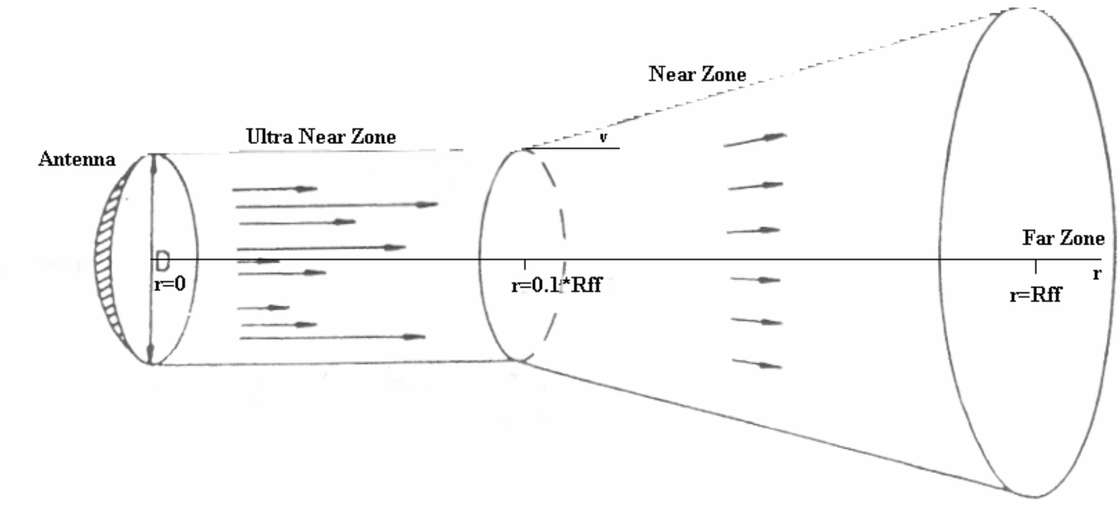

Figur 2.2. *Model for the power density along an antennas radiation axis.*

The power density is given by

$$\rho(r) = {P_t}/{A(r)}$$

where P_t is transmitted effect and A(r) is the area across the axis. If the main lope of the antennas is 2*vº (3 dB points), is the power density in the three zones given by r:

Ultra near zone, r < 0,1 R_{ff}

$$\rho(r) = P_t / \pi(\tfrac{1}{2}D)^2 \quad [W/m^2]$$

Near zone, 0,1R_{ff} < r < R_{ff}

$$\rho(r) = P_t / \pi\left(\tfrac{1}{2}D + (r - 0.1R_{ff})\tan V\right)^2 \quad [W/m^2]$$

Far zone, R_{ff} < r — Gaussian distribution of the power

In figure 2.3 the decrease in power density as a function of distance is calculated.

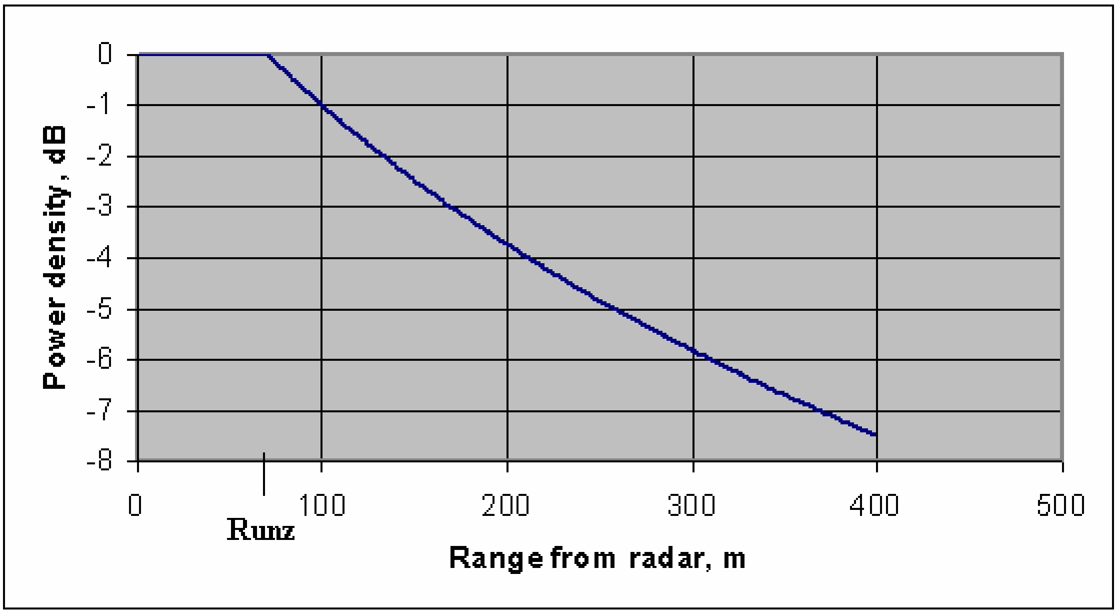

Figure 2.3. *Power density as a function of distance from the radar, calculated for a 4,2 m reflector at C-band.*

Any blockage of wind mills in the ultra near zone and near zone should not take place, but even in the closer part of the far zone, wind mills have a great effect on the propagation of electromagnetic energy. This is shown in the Météo France study referred below.

A study of the impact of wind mills, Météo France has been studying the potential impact of such projects on weather radars, focusing on 3 different scenarios:

- Blocking of the beam
- Clutters
- Doppler

From this study, the main results in terms of impact on radar data have been extracted in the following.

Impact of beam blocking

The masking of the radar beam by one or more wind turbines blames measurements on the considered azimuth angles, i.e. when the radar points in direction of the wind turbine.

For a wind turbine and according to the type of radar, these angles range between 1 and 2 degrees that can represent significant geographical areas for which hydro-meteorological measurements can be erroneous, as described on figure 2.4 below.

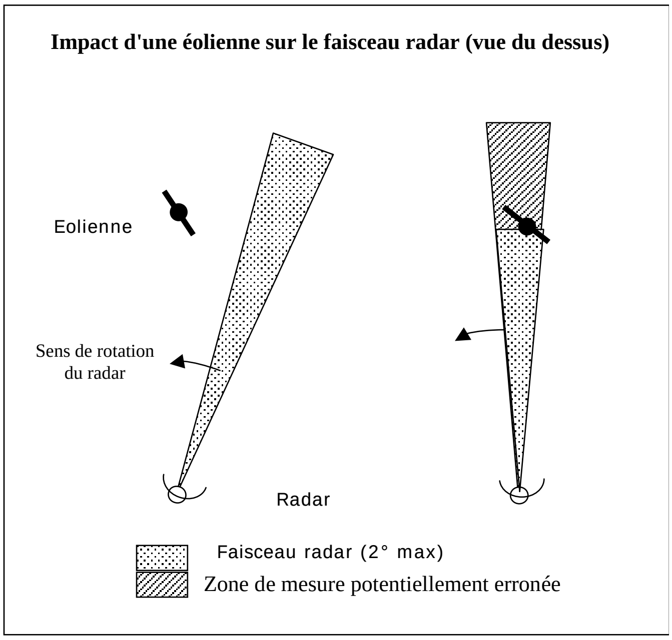

Figure 2.4: *Impact of a wind turbine on radar beam (from the above)*

The following analysis was carried out with radars implemented at 20 meters height and presenting 1 and 2° beam aperture (at 3 dB), typical of weather radars in France and for two types of wind turbines showing the following characteristics:

Type 1:

- 70 meters height shaft
- section from 4 to 2 meters
- 3 blades of 40 meters length and 2 meters broad

Type 2:

- 120 meters height shaft
- section from 6 to 4 meters
- 3 blades of 70 meters length and 3 meters broad

On this basis, figures 2.5 and 2.6 below give the values of percentage of the radar beam blocking according to the distance to the wind turbine and show that, in the event of direct line of sight between the radar and the wind turbine, even beyond a 2000m distance (representing the regulatory protection of radars in France), only one wind turbine has the potential to block, in the considered azimuth, more than 10% of the radar beam and until a few % to 10 km. Considering, in addition, that several wind turbine are in general installed in the same farm, one can legitimately estimate, according to their fitting, that the impact of such installations remains critical until a distance of 10 km, in particular for the radars presenting an opening at 1° (C Band mainly).

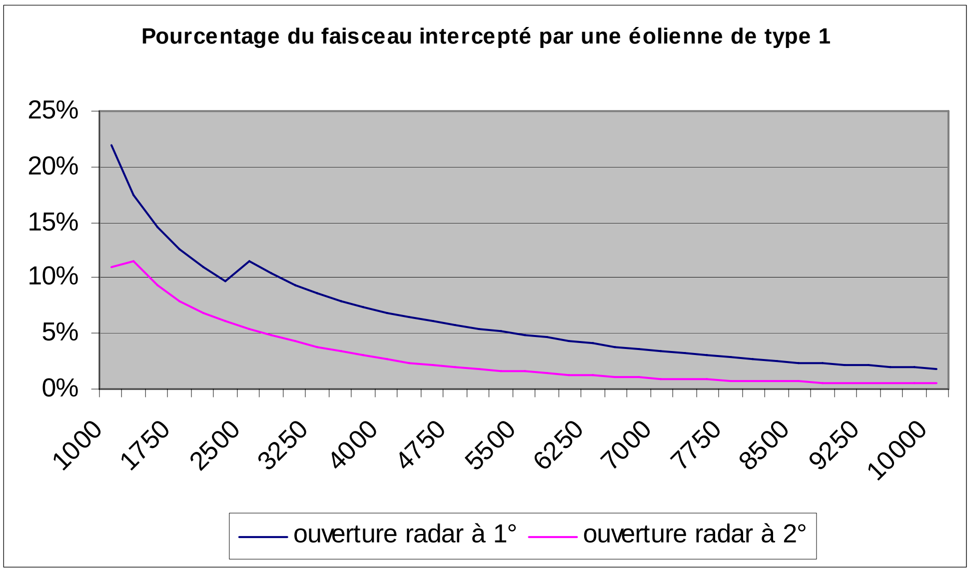

Figure 2.5: *Percentage of radar beam blocking by a type 1 wind turbine vs distance*

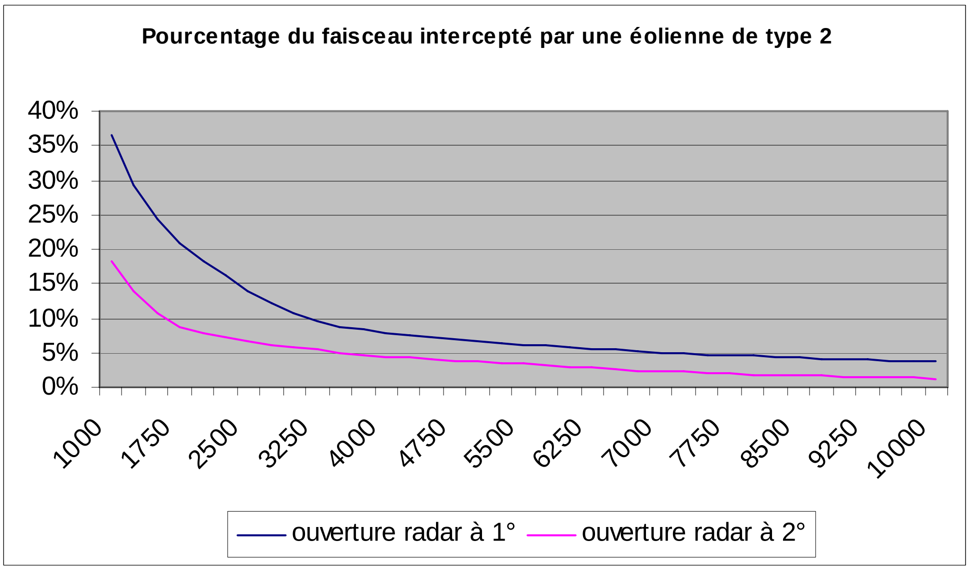

Figure 2.6: *Percentage of radar beam blocking by a type 2 wind turbine vs distance*

Impact of the clutter

Weather radars perform precipitation measurements expressed in reflectivity (dBz). These radars are calibrated in order to coincide with the level of noise of the receiver with the 0 dBz reflectivity level at 100 km. In addition, the minimal detection level of a rain cell is fixed at 8 dBz.

To determine the impact of the clutters produced by the wind turbines requires the knowledge of Wind turbines Radar Cross Section (RCS) (*"Surface équivalente Radar" (SER) in French, as mentioned of several figures below)*, which is not a trivial task and depends on the specific characteristics of the wind turbines.

There exists however in the literature a certain number of generic elements, and in particular the English study relating to the aeronautical radars handled by Qinetics ("Wind farm impact on radar") that gives a range of RCS from 200 to 2000 m² (i.e. 23 to 33 dBsm) for the wind turbines, taking into account both shaft and blades.

At all distances up to 30 km, the level of detection of the wind turbine is largely higher than the minimum level of reflectivity (8 dBz) and higher, in almost all cases, than the saturation threshold (64 dBz). An clutter will thus be produced by the wind turbine in all cases.

In the horizontal plane, taking into account the rotation of the radar, this clutter will endure as much as the discrimination of antenna between the main lobe of the antenna and the direction of the wind turbine will not bring back the level of detection of the wind turbine below the minimum level of reflectivity (8 dBz).

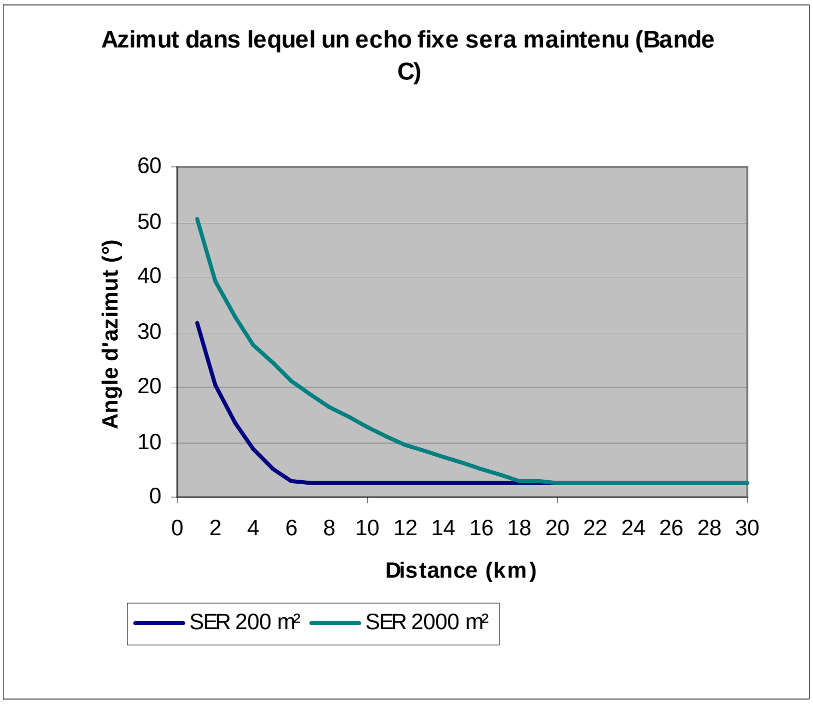

Figure 2.7: *Azimuth in which a wind turbine clutter will be maintained (C band)*

It thus appears that, in the case of wind turbines presenting RCS ranging from 200 to 2000 m², the clutter produced by the wind turbine will be present in very significant azimuths (several tens of degrees) compared to the direction of the wind turbine, even at quite large distances. At least, beyond respectively 6 and 18 km, the impacted azimuth is about 2°.

Taking into account on the one hand the detection grid of the weather radars presenting pixels of 1km x 1km, and on the other hand link effects (the pulse detection of the wind turbine will likely cover 2 contiguous pixels), one can then calculate the number of pixels which will be made unusable because of the Clutters products by the wind turbine (see figure 2.8).

The clutter produced by a wind turbine will be maintained as given in figure 2.7.

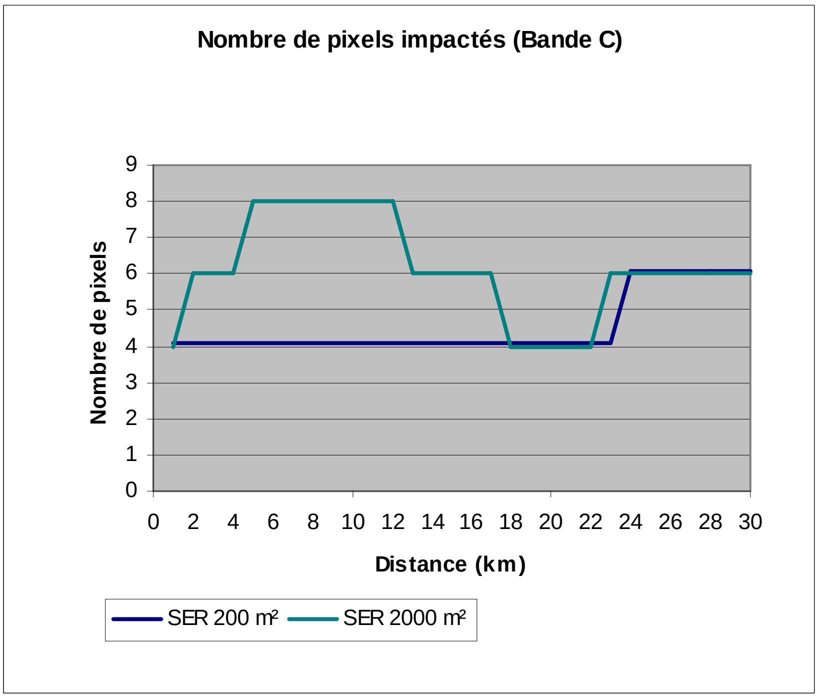

Figure 2.8: *Number of impacted pixels (C band)*

Impact in Doppler mode

Unlike for reflectivity (in dBz) which is a measurement of intensity of the signal, Doppler detection is carried out on the phase of the signal and thus takes place as soon as the received signal is higher than the level of noise (i.e. -113 dBm).

For the determination of the impact on the Doppler mode, only the blades, moving, are to be taken into account. It is hence obvious that Radar Cross Section (RCS) to be considered are much lower than the total RCS of the wind turbine and a range of 5 to 10% ratio has been used. On this basis, the RCS considered in the analysis have been taken between 10 and 200 m² (10 dBsm to 23 dBsm), respectively corresponding to 5% of 200 m² and 10% of 2000 m².

Compared with the "Clutters" scenario and taking into account the obvious spectral correlation between the measurement of wind and the echo of the wind turbine, one can thus estimate that the

Doppler mode will be more sensitive to the effect of the wind turbines, in particular at short distances, as shown on figure 2.9 below.

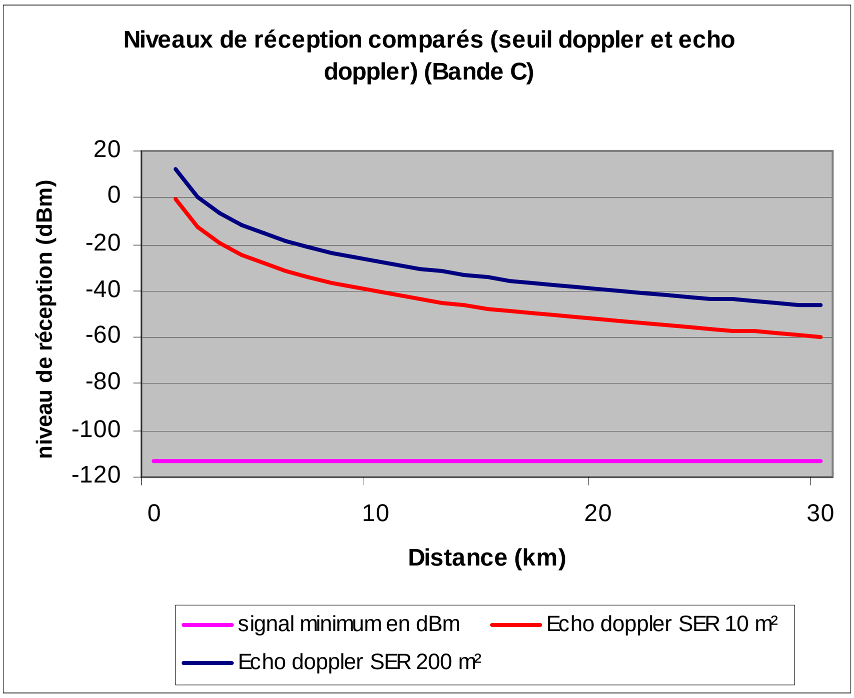

Figure 2.9: *Compared receiving levels (Doppler threshold and Doppler Echoes) (C band)*

At all distances up to 30 km, one can see that the level of detection of the wind turbine is largely higher than the level of Doppler detection (-113 dBm), between 50 and 120 dB and that thus, in all cases, the Doppler treatment will be disturbed.

In the horizontal plane, taking into account the rotation of the radar, this Doppler echo will endure as far as the discrimination of antenna between the principal lobe of the antenna and the direction of the wind turbine will not bring back the level of detection of the wind turbine below the level of minimal detection (-113 dBm).

The azimuths in which a Doppler echo will be maintained are given on figure 2.10.

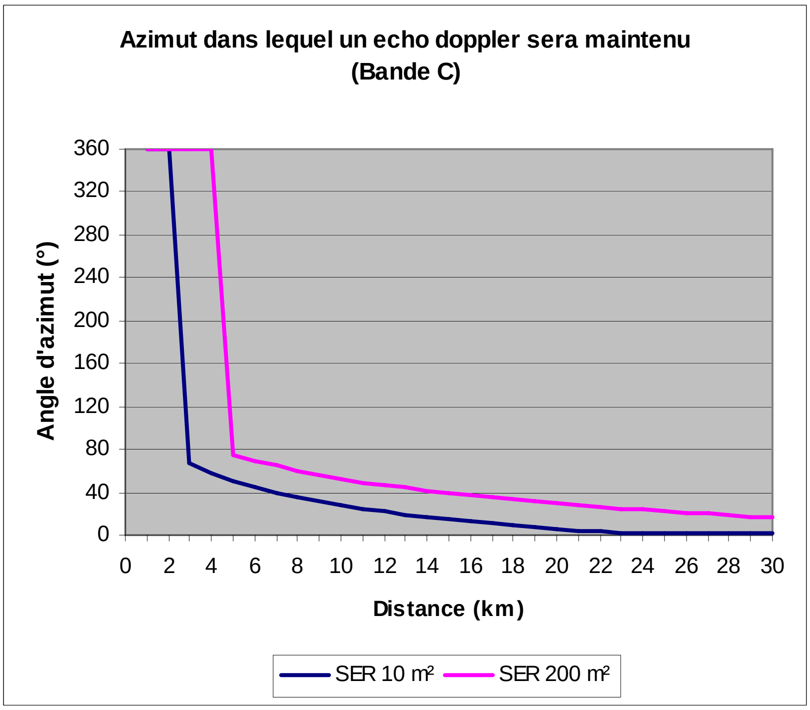

Figure 2.10: *Azimuth in which a wind turbine Doppler echo will be maintained (C band)*

It thus appears that, in the case of wind turbines presenting Doppler RCS from 10 to 200 m², the impact on the Doppler treatment will be present at all azimuths and elevations for a wind turbine located until, respectively, 2 and 4 km. This extreme situation is explained by the fact that in this case, the maximum antenna discrimination (in the side lobes and even in the back lobes) is not sufficient enough to attenuate the Doppler signal received from the wind turbine.

For the other distances, the values of impacted azimuths remain very high (several tens of degrees), blocking measurement on significant geographical areas for which, in addition, all elevations will be impacted, only reaching lower values than 3° beyond 22 km.

There still, taking into account on the one hand the detection grid of the weather radars presenting pixels of 1km x 1km, and on the other hand link effects (the pulse detection of the wind turbine will likely cover 2 contiguous pixels), one can then calculate the number of pixels which will be made unusable because of the Doppler echoes produced by the wind turbine (see figure 2.11).

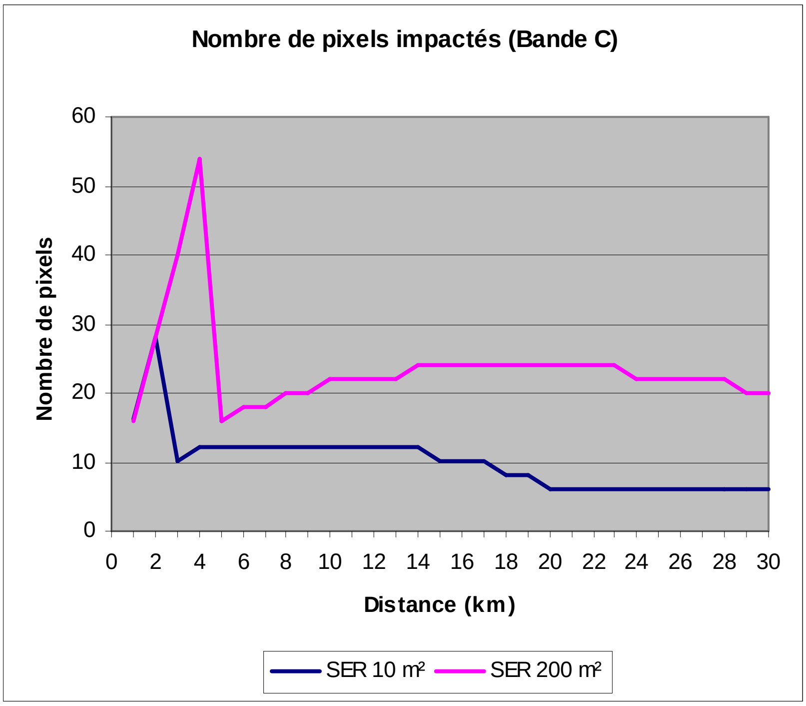

Figure 2.11: *Number of impacted pixels (C band)*

The number of impacted pixels is thus very large, in particular at short distances, and remains sufficiently significant, including beyond 20 km, for potentially calling into question the whole of Doppler measurements.

4. Météo France

Jean-Luc Chèze, December 2006.

I - Example of the angular range of the perturbation due to sidelobes

The size of the areas where the signal processing is perturbated in Doppler mode can be large due to the fact that we need to treat signals of low levels in clear air conditions. In such a case, the perturbation can occur when the obstacle is intercepted by the main lobe, but also by the side lobes.

This example illustrates this effect on the case of clutter returned by boats on the Channel. Using radar data codes on 80 levels, it was possible to visualize pixels of high reflectivity (dark red for 56 dBz) for the example but also pixels of very low reflectiviy close to –5 dBz (in dark blue).

In this example, a boat generates clutter on an angular sector of approximatively 20 degrees at a range of 71 km.

It is interesting to notice that the maximum reflectivity of 56 dBz correspond to a RCS (Radar Cross Section) of 10000 m^2 at 71 km and that our model (see figure 3.1) gives an azimuthally angular amplitude of 20.2 degree for the perturbation, confirmed by the observation.

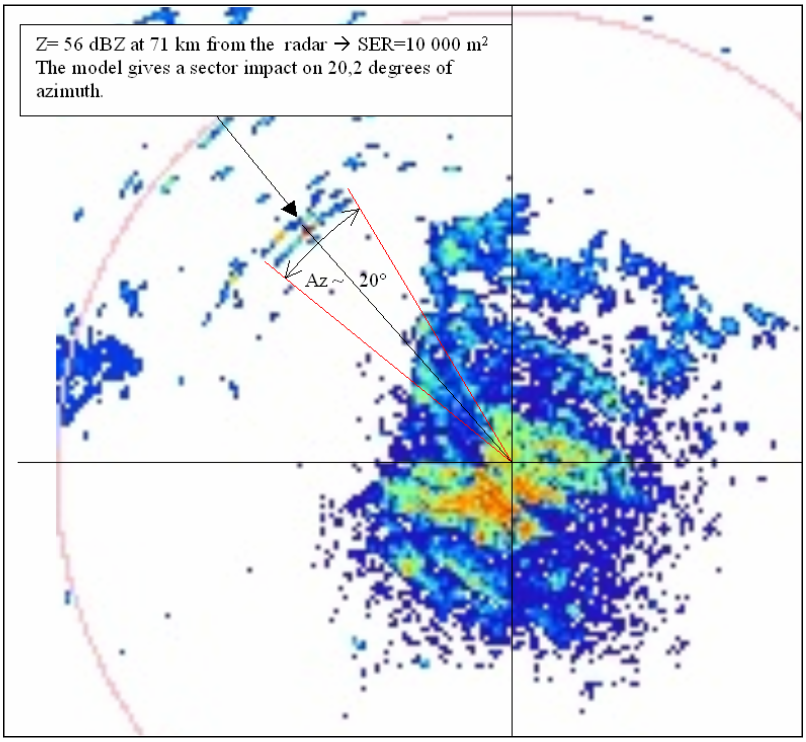

Figure 3.1: *Abbeville radar on 5 March 2006 at 21h20 TU (22h20 loc), image of reflectivity with a spatial resolution of 1km coded on 80 levels (site 0,4°). Clutters that appear at ranges from about 60 to 80 km are due to boats on the Channel.*

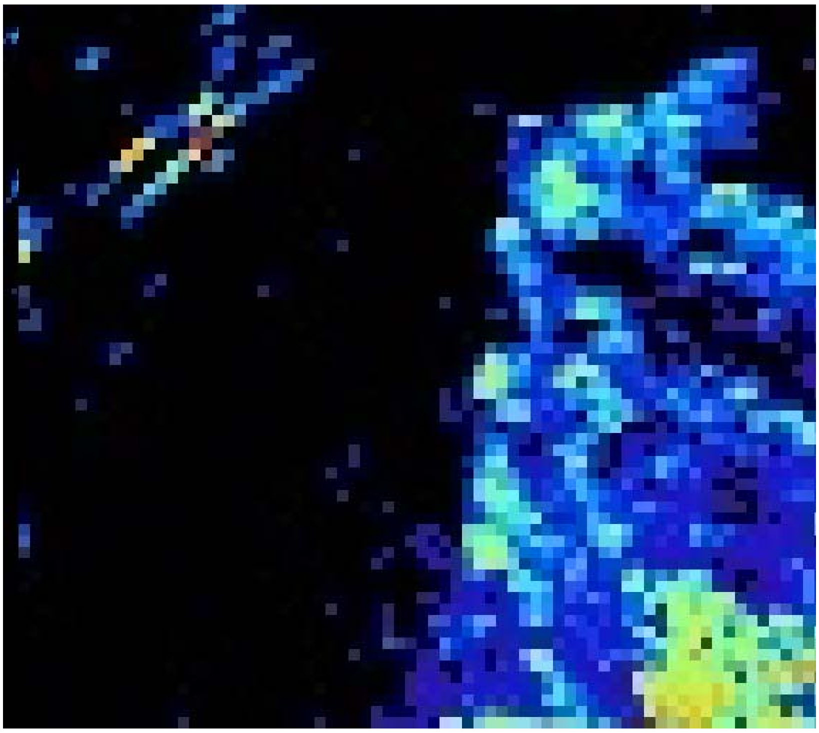

Figure 3.2: *(Extract from figure 3.1) The maximum of reflectivity is 56 dBz (dark red) at 71 km ; it corresponds to RCS of 10000 m^2.*

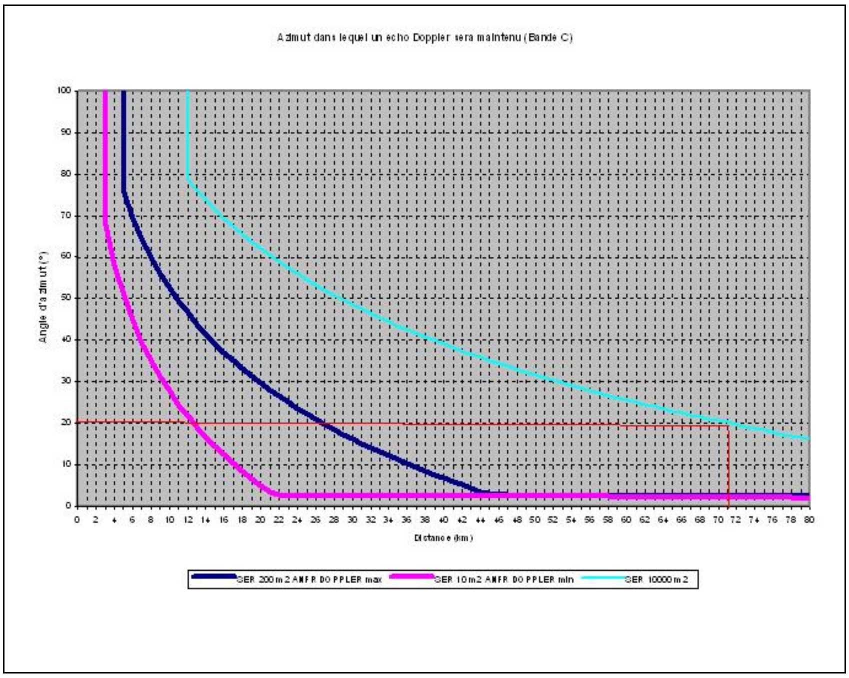

Figure 3.3: *The maximum reflectivityl of 56 dBz at 71 km corresponds to a RCS of 10000 m2 ; for this values, the model gives an azimuthal impact of 20,2°, close to the observed value.*

II - Example of clutter due to windmills

A windfarm, that has been installed in the village of Nibas, gave the opportunity to have measurements of the clutter induced for our Abbeville radar.

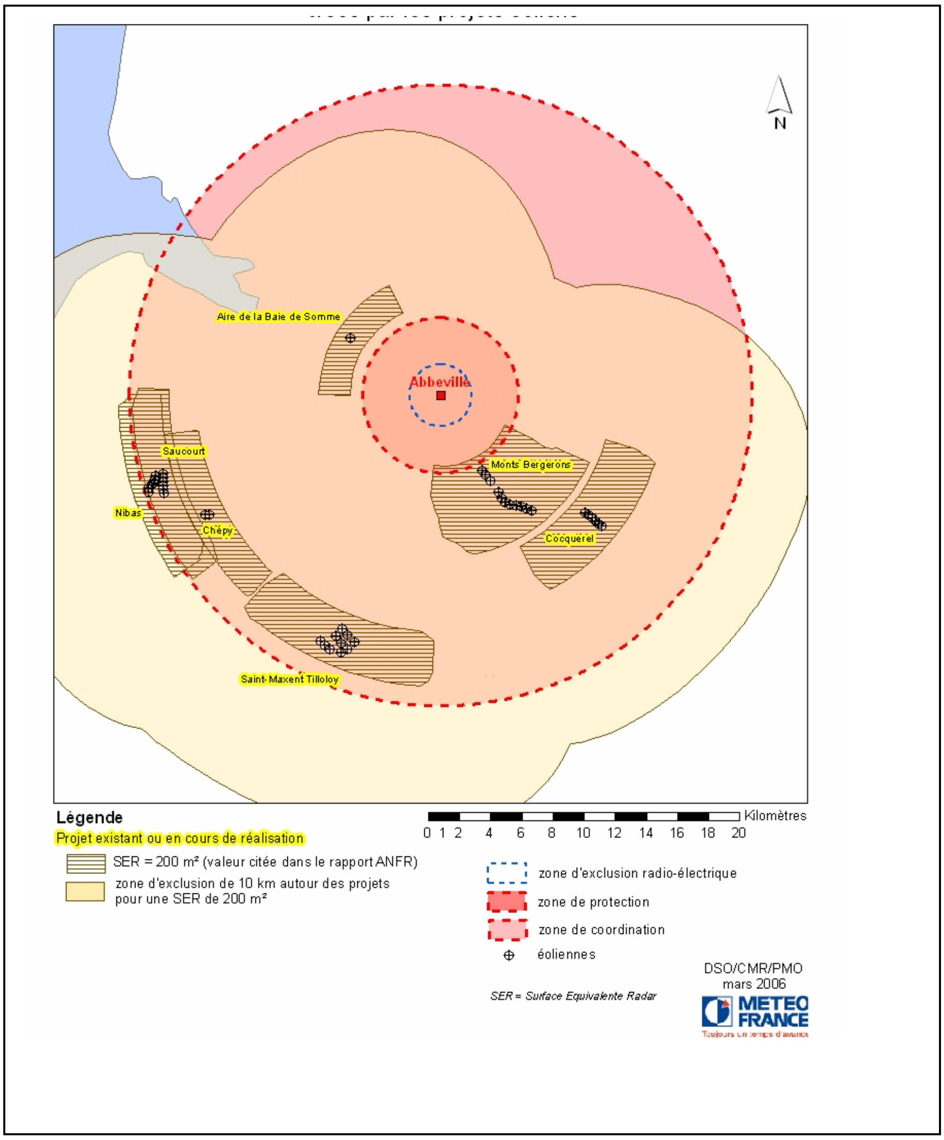

Figure 3.4: *Existing wind farms or projected in the vicinity of the Abbeville radar.*

The windmills are at a range of 17-19 km in the WSW of the radar (see figure 3.4). The figure 3.5 gives the characteristics of the windmills.

The distribution of the values of the reflectiviy for the 6 pixels of the images of the Abbeville radar concerned by the windmills has been plotted on the figure 3.6. The reflectivity ranges from about 45 to 60 dBZ for the majority of the pixels and presents a fluctuation of amplitude of 15 dB due to the fact, that the RCS varies when the blades are rotating.

From this example, it is possible to conclude that the order of magnitudes of the echoes induced by the windmills is coherent with the theoretical study included in this report.

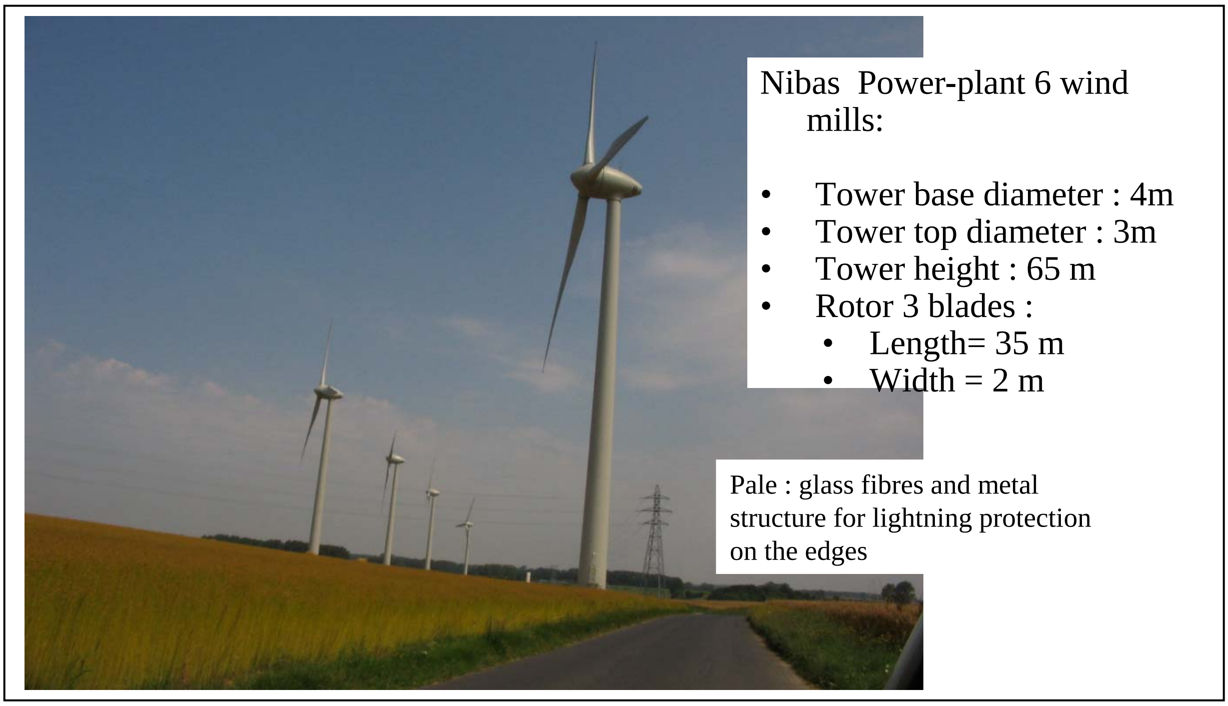

Figure 3.5: *Characteristics of the windmills of the Nibas windfarm.*

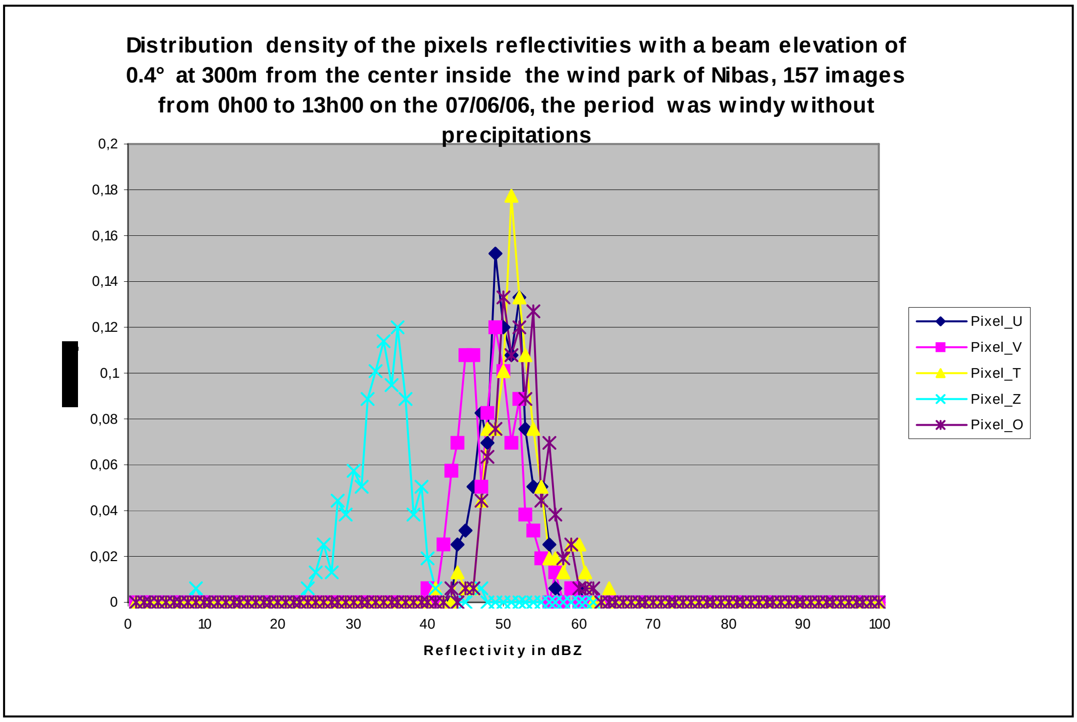

Figure 3.6: *Distribution of reflectivity for the pixels corresponding to the Nibas windfarm*

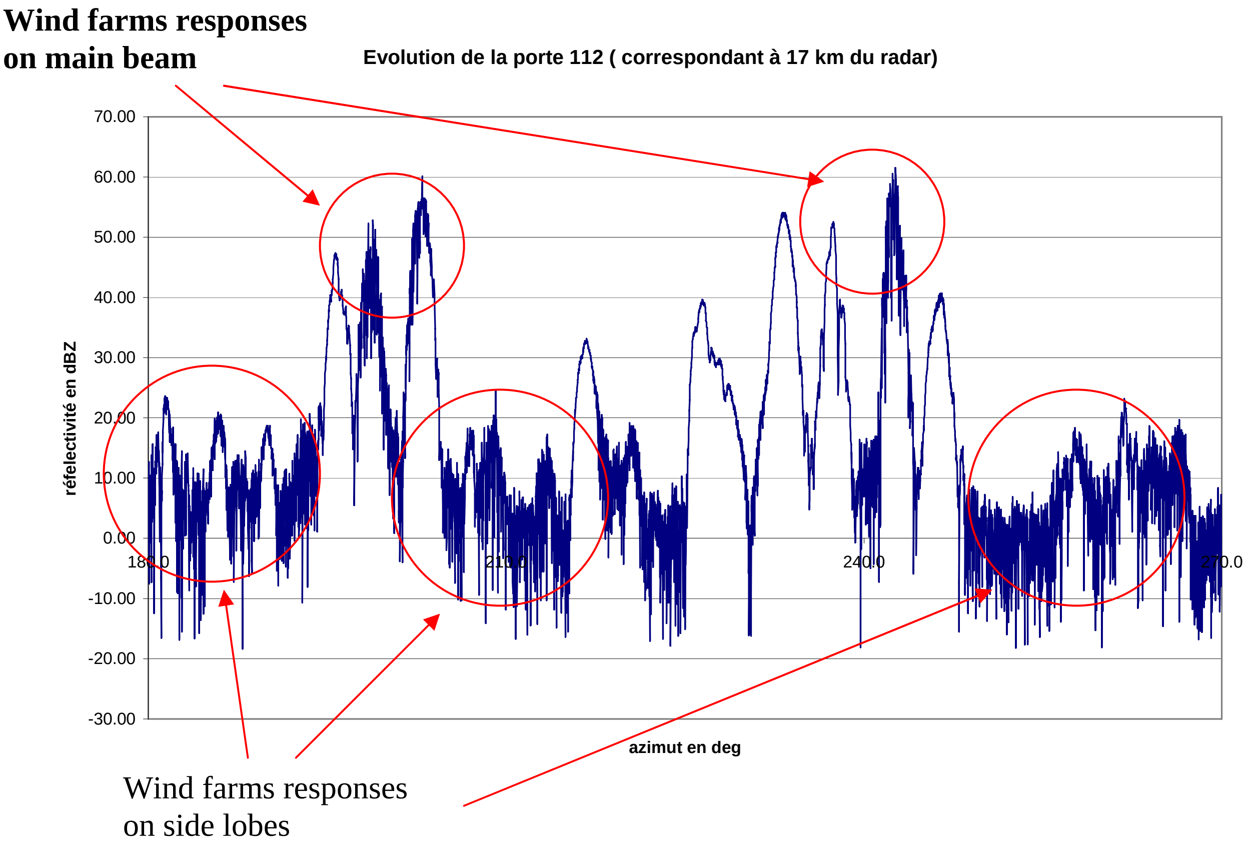

Figure 3.7 *Dynamic measurements of wind farms impact*

Figure 3.7 shows the dynamic measurements of wind farms impact at The Abbeville Radar, corresponding to the received signal without any filtering.

It corresponds to the gate 112 at 17 km from the radar over an azimuth of 90°.

At a first glance, it confirms the huge dynamic of wind farms responses, due to blade movement. Considering the wind farms responses in the main beam, it still confirms the equivalent RCS of about 23 dBm.

Considering the other azimuths, it obviously shows the huge wind farms impact through side lobes with signal in the range –10 /+20 dBz, i.e. between 5 and 35 dB above the radar sensitivity that is roughly at –15 dBz at 17 km.

Relating this to Doppler measurements that are performed right above the radar sensitivity confirms the high potential threat of wind farms on Doppler products over very large area.

5. KNMI

Iwan Holleman, KNMI, 6 December 2006 (Photos: Paulien van Eif)

Introduction

Within the OPERA (Operational Programme on the Exchange of RAdar data) programme of EUMETNET a project on the Impact of Wind Turbines on Weather Radar data is conducted. The impact on both the reflectivity data and Doppler data is assessed in this project using observed volume data and theoretical calculations. As a first step cases of co-existing wind turbines and weather radars are collected and documented.

Radar "Den Helder" of KNMI

KNMI operates two identical C-band Doppler weather radars from Gematronik GmbH. One radar is located in De Bilt (52.10N,5.18E) and the other one in Den Helder (52.96N,4.79E). The locations of the two radars are shown on the map in Figure 4.1. The circles indicate a range of 150 km from the radar sites which is roughly the maximum range for quantitative use of the data. The received signal is digested by a RVP6 radar processor (Sigmet Inc, www.sigmet.com) and the generation of radar products is done with the Rainbow package (www.gematronik.com). The radar in Den Helder is located at a naval airbase which is almost completely surrounded by sea. This "windy area" is rather popular for wind turbines and four wind turbines are located within 1 km from the radar. Many building applications for additional wind turbines have been rejected by KNMI because of the expected performance loss of the radar system. In the right map of Figure 4.1 the Den Helder radar site is displayed together with the locations of the four wind turbines. The geographical coordinates and heights of the radar antenna and wind turbine housings are listed in Table 1.

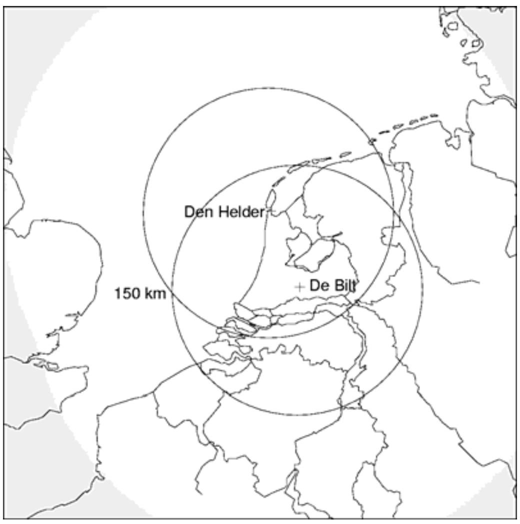

Figure 4.1: *A map of the Netherlands with the locations of the two weather radars (left) and map of Den Helder radar site with wind turbine locations (right).*

Name	Height [m]	X [km]	Y [km]	Dist. [km]	Azim. [deg]
Radar Den Helder	51	114.900	551.910	0	0
Helsdeur 1	48	114.830	551.250	0.665	185.6
Helsdeur 2	48	114.762	551.141	0.781	190.2
Ambachtsweg 1	30	114.300	550.800	1.261	207.9
Ambachtsweg 2	30	114.300	550.650	1.394	205.0
Het Nieuwland	40	112.470	551.450	2.466	258.8

Table 1: *Coordinates and heights of the radar antenna and wind turbine housings. The two left columns give the distance and azimuth of the object from the Radar Den Helder.*

Wind Turbines at "Helsdeur"

The two wind turbines at Helsdeur are located closest to the radar at a distance of only 665 meters. The height of the housing is about the same as that of the radar antenna. The wind turbines are approximately south of the radar at azimuths of 186 and 190 degrees. The height of the wind turbine housing is 48 meters. The maximum cross section of the turbine housing is 21 square meter and the diameter of the blades is 50 meter.

Figure 4.2: *Photo of the two wind turbines at "Helsdeur". Note that the radome of the Den Helder radar is just visible above the corner of the building right of the closest turbine tower.*

Wind Turbines at "Ambachtsweg"

The two wind turbines at Ambachtsweg are located between 1200 and 1400 meters from the radar in Den Helder in south-westerly direction. The housings of the wind turbines are somewhat lower than the radar antenna but they still may influence the lower half of the radar beam.

Figure 4.3: *Photo of the two wind turbines at "Ambachtsweg".*

Wind Turbine at "Het Nieuwland"

The wind turbine at Het Nieuwland is located at roughly 2.5 km from the radar in westerly direction. Because the wind turbine is located about 2.5 km from the radar and also is about 10 meter lower than the radar antenna a minor impact (if any) is expected for this wind turbine.

Figure 4.4: *Photo of the wind turbine at "Het Nieuwland".*

Reflectivity data from radar Den Helder

An example of raw reflectivity data of radar Den Helder from the lowest elevation (0.3 degrees) is shown in Figure 4.5. At short ranges intensive sidelobe clutter can be seen around the radar location both above land (south and north of radar) and sea (west and northeast of radar). Note that the location of the weather radar is marked with a cross. Precipitation is observed north and east of the radar. No additional or amplified clutter is seen in the direction of the wind turbines (186 – 260 degrees azimuth) in this single radar image.

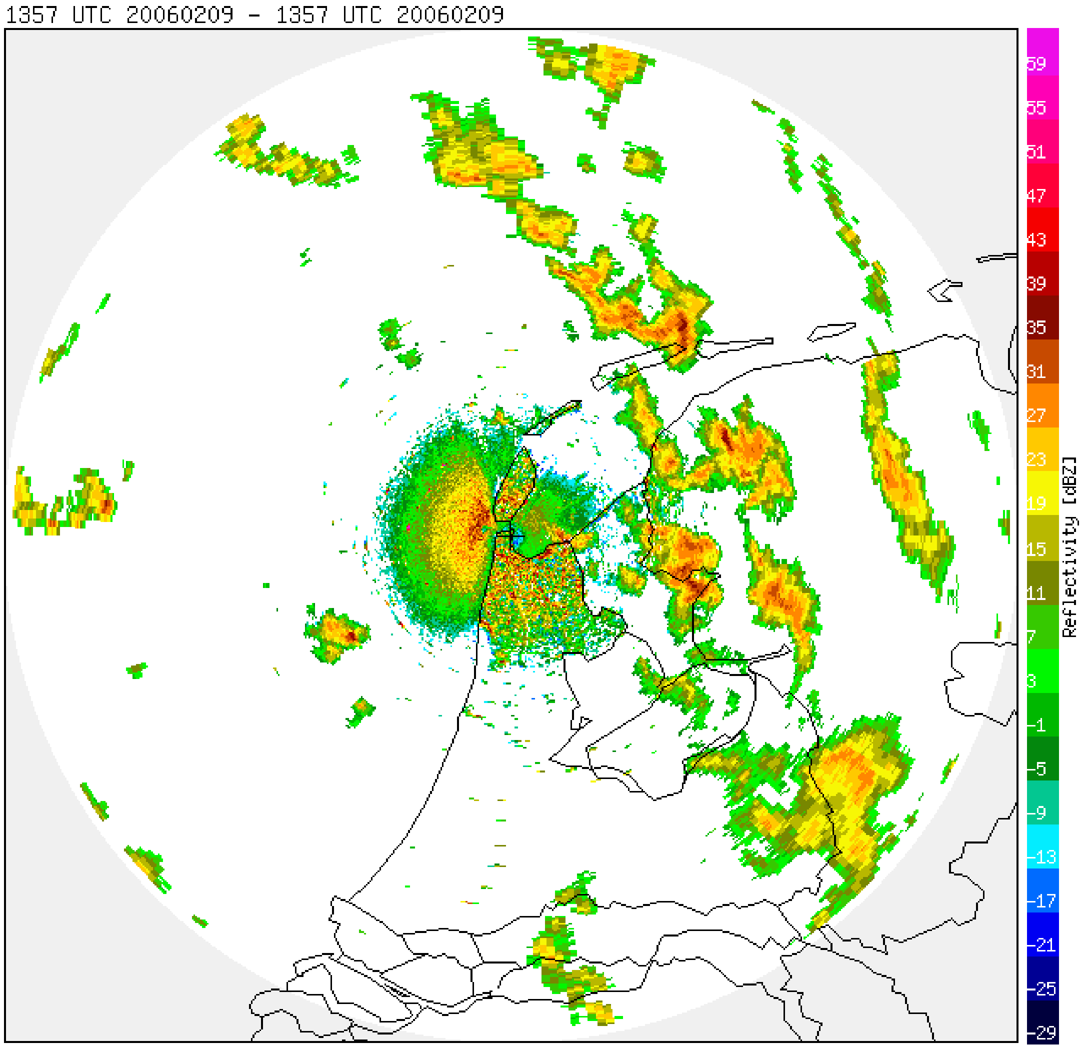

Figure 4.5: *Reflectivity data from lowest elevation (0.3 degrees) of radar Den Helder. The location of the radar is marked with a cross.*

Doppler data from radar Den Helder

An example of Doppler data of radar Den Helder from the lowest elevation is shown in Figure 4.6. The green pixels correspond to areas with zero Doppler radial velocity and thus are precipitation areas which are moving perpendicular to the radar or ground/sea clutter. At short ranges intensive sidelobe clutter can again be seen around the radar location both above land (south and north of radar) and sea (west and northeast of radar).
Note that the sea clutter has a slight positive radial velocity indicating that the sea surface, i.e. the wind induced waves, are moving towards the radar. No additional or amplified clutter is seen in the direction of the wind turbines (186 – 260 degrees azimuth) in this single Doppler radar image.

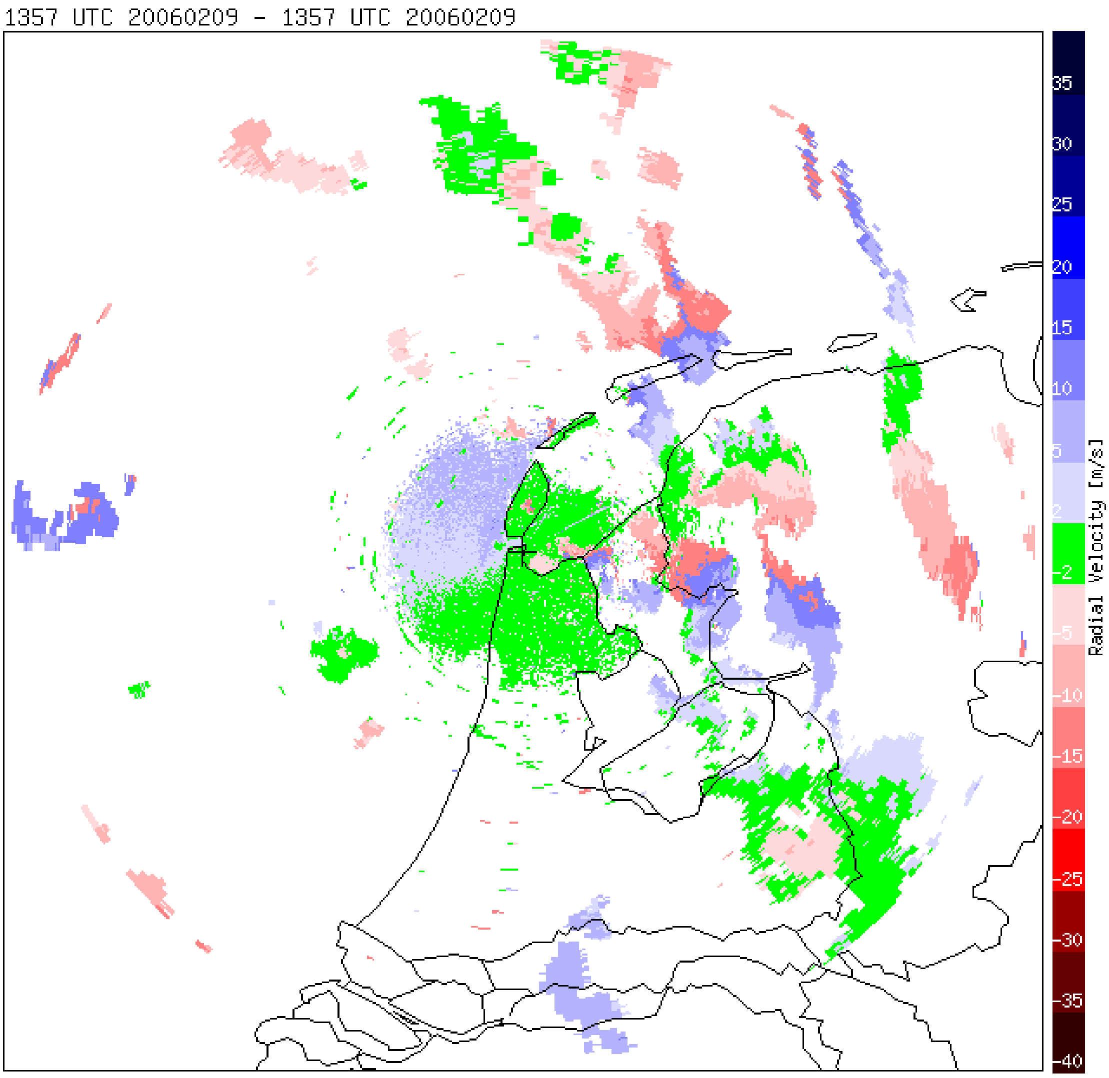

Figure 4.6: *Doppler data from lowest elevation (0.3 degrees) of radar Den Helder. The location of the radar is marked with a cross.*

Accumulated data from radar Den Helder

An example of accumulated precipitation data from radar Den Helder for whole December 2005 is shown in Figure 4.7. The accumulation product is based on pseudoCAPPI products at 800 meter altitude and has not been corrected with gauges. The range dependence of the observed precipitation is obvious and is mainly due to a non-uniform vertical profile of reflectivity. Several irregularities in the accumulated precipitation can be seen at longer ranges often due to tall buildings around the radar site, but also the effect of the wind turbines Helsdeur can be seen in southerly direction. The Helsdeur turbines are closest to the radar and are also the tallest wind turbines around the radar.

The disturbances can be better in Figure 4.8 which shows the mean precipitation depth as a function

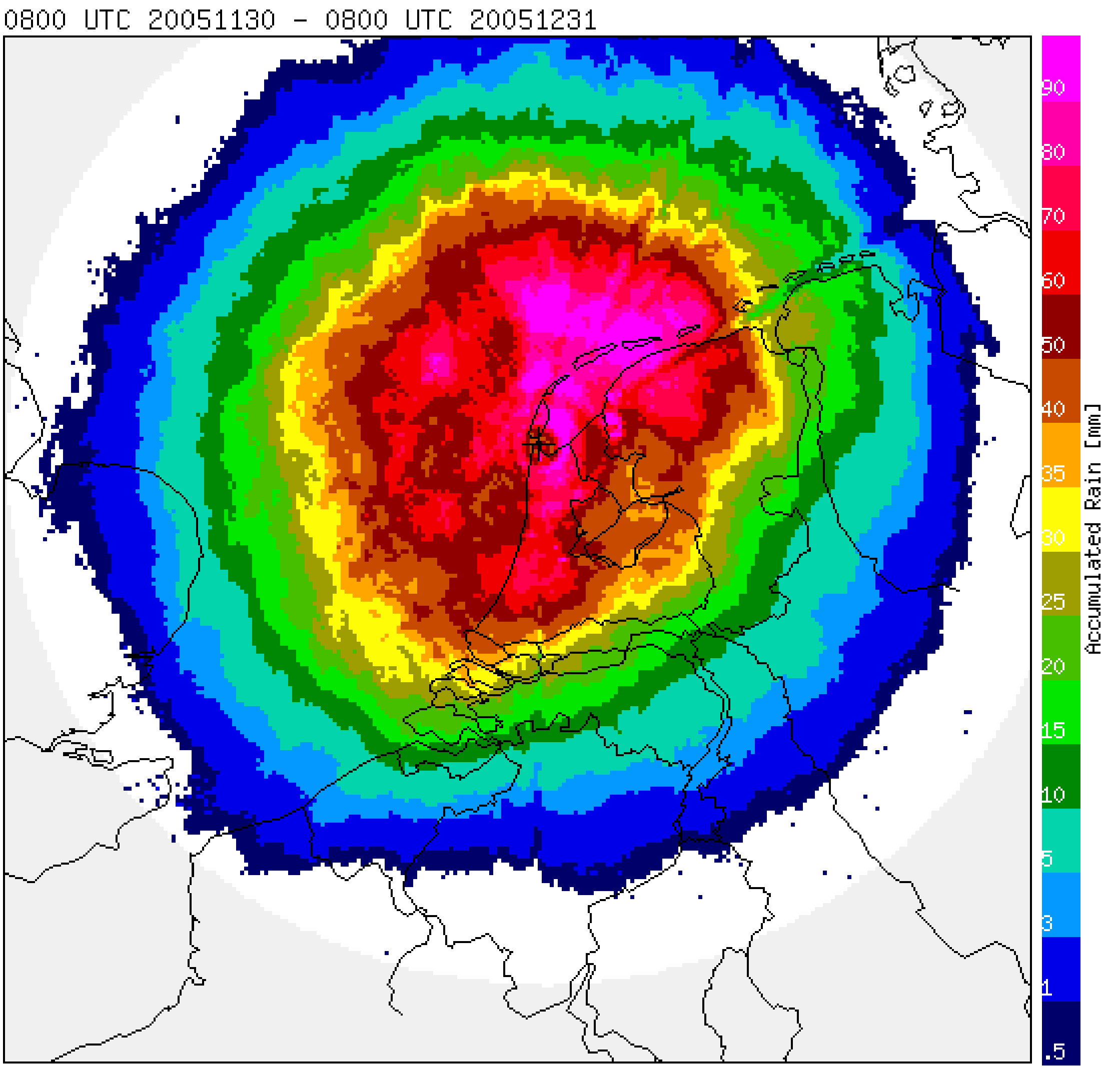

Figure 4.7: *Accumulated precipitation product from the radar Den Helder for whole December 2005. The location of the radar is marked with a cross. The accumulation product is based on pseudoCAPPI products at 800 meter altitude and has not been corrected with gauges.*

of azimuth. The mean precipitation depth is calculated by recalculating the azimuth with respect to the radar for each Cartesian pixel in the accumulated precipitation product and collecting the data in 1 degree bins. The mean precipitation varies between 10 mm (in southeast direction) and 35 mm (in north direction). **Several disturbances can be seen due to blockage by buildings and the disturbance by the wind turbines at Helsdeur is indicated in the figure.**

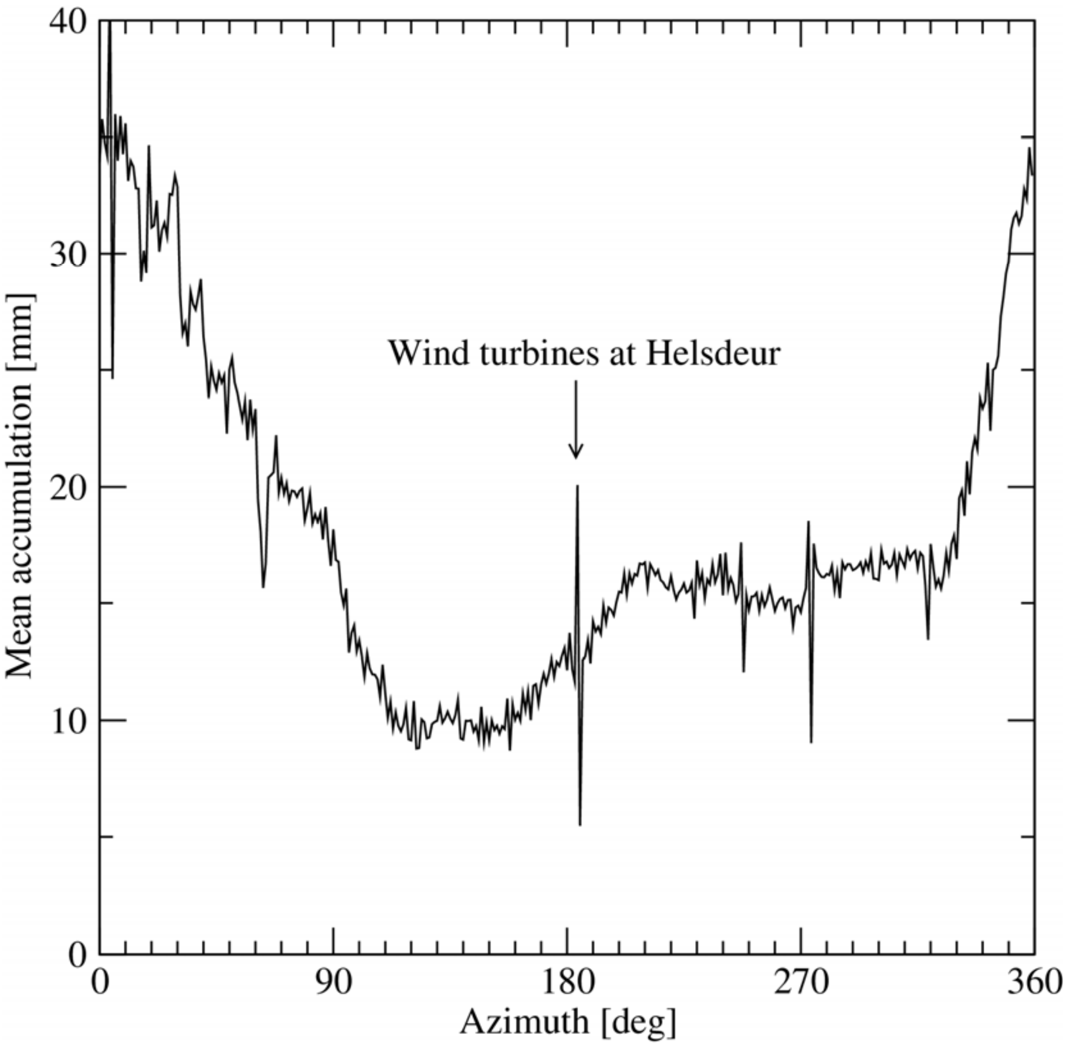

Figure 4.8: *Mean accumulated precipitation as a function of azimuth calculated from the accumulation product shown in Figure 7.*

6. INM

Fernando Aguado, December 2006.

Examples of Spanish radar beam blocking. Both are produce by phone-mobiles antennas.

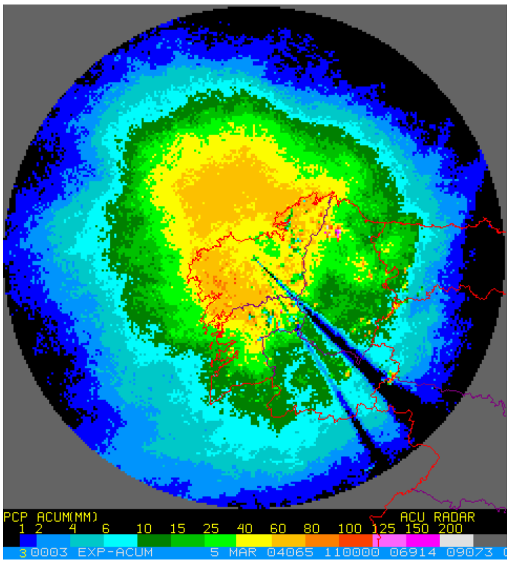

Figure 5.1: *Ocurrences of rain. Radar of Cerceda. March, 2004*

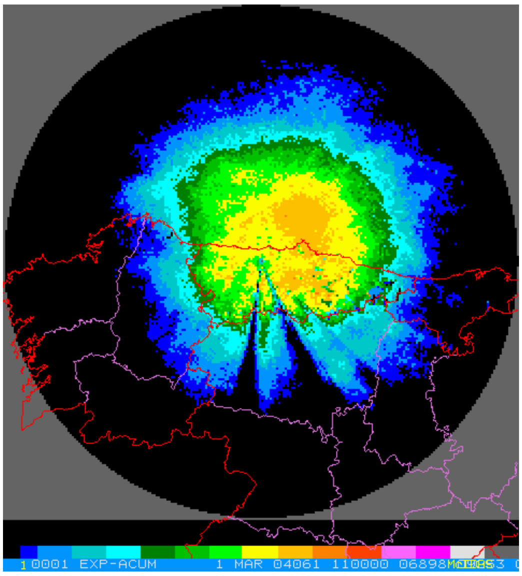

Figure 5.2: *Ocurrences of rain. Radar of Aguión. March, 2004*

7. DWD

P. Lang and S. Hafner, December 2006.

The Nysted offshore wind park south of the Danish island Lolland is covered by 72 wind turbines with 70m high propellers each. An example is shown on figure 6.1.

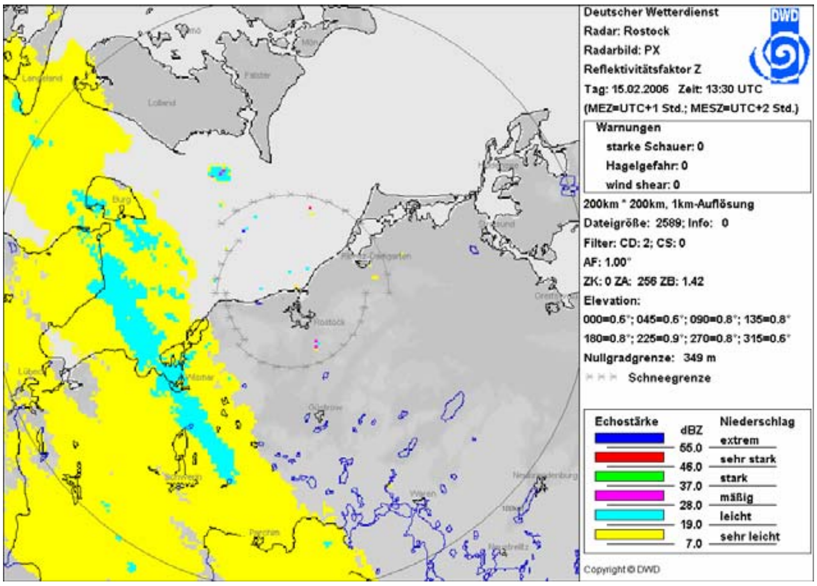

Figure 6.1: *Reflectivity data from the Rostock weather radar showing the Nysted windmill farm.*

The 48 km distant wind park is usually visible in radar products during normal sea surface propagation of the radar beam (Rostock Radar). The best way to isolate these ground echoes is provided by using accumulation products of several hours (figure 6.2). Here also the shipping routes are visible, which also go back to moving or rotating non- weather echoes such as wind turbines (figure 6.3).

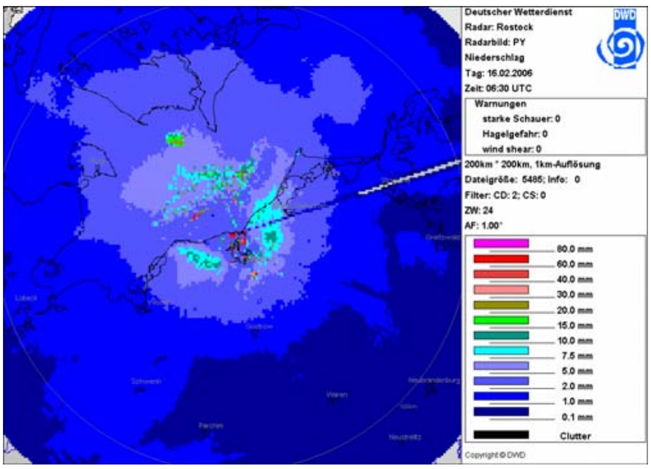

Figure 6.2: *Accumulated data from Rostock weather radar.*

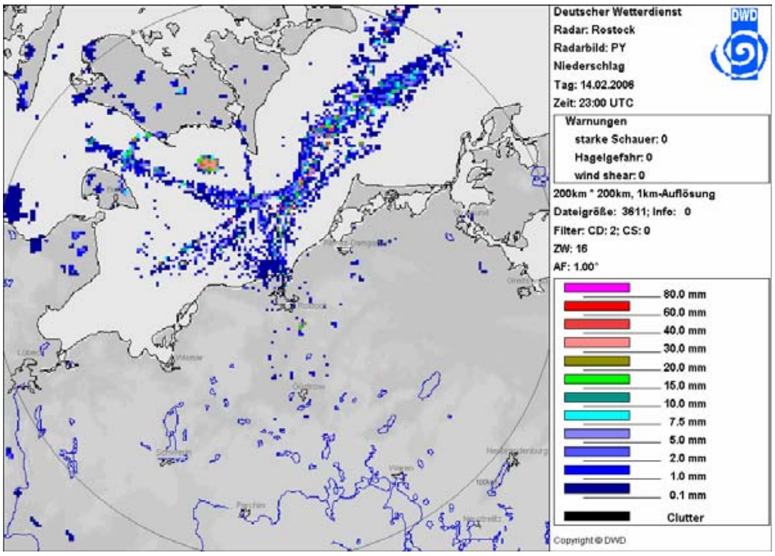

Figure 6.3: *Shipping routes in the southern Baltic Sea.*

In the Nysted case, there is often anomalous Doppler behaviour at the park site was detected (figure 6.4). This leads to the question in which sense and direction the combined rotor signal is maximising. Further concepts concerning the combined rotor radial wind direction and chances for filtering must be designed. As even weak wind prevent Doppler filtering, only few cases of ground clutter recognition are probable.

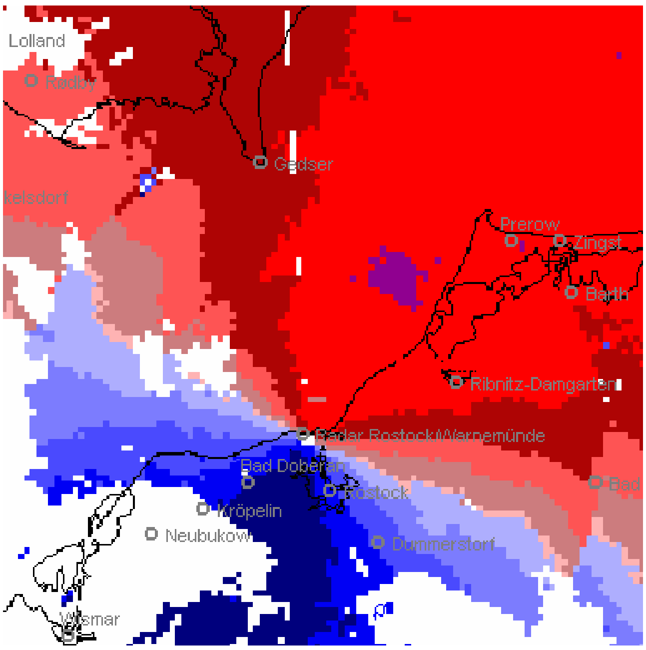

Figure 6.4: *Doppler data from Rostock weather radar.*

The basic idea is the treatment of wind parks as weather echoes due to non-typical velocity or drift identification. Only in calm situations the stopped rotors have their expected ground clutter identity.

In the second case the windmill farm is within the 8km distance of the weather radar Emden (figure 6.5). Here some pixel of 24h pseudo rain is accumulated to more than 40mm while echoes of 30-40 dBz are reached (figure 6.6). Here no clear Doppler anomalies were found in the few case studies.

Figure 6.5: *The windmill farm near Emden.*

The 14 km distant wind park near Radar Ummendorf (figure 6.7) shows a constantly strong echo accumulation near 30-40 dBz and sums of > 60mm/24h. There also the Doppler behaviour is not uniform.

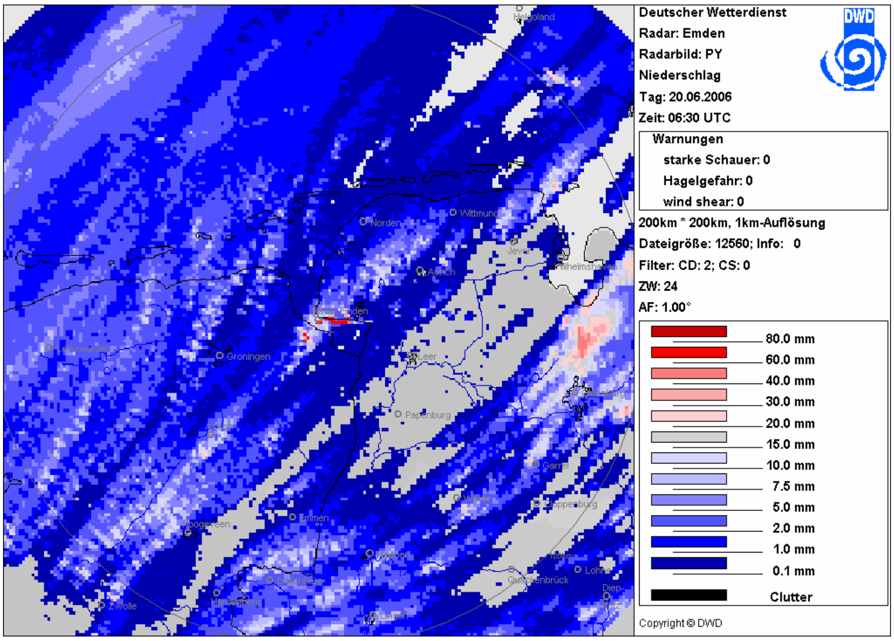

Figure 6.6: *Reflectivity data from the windmill farm near Emden*

Some other wind parks near the A44 Autobahn north of Marsberg are estimated as essential, but do not show more than weak temporary echo effects on the 24km distant Flechtdorf Radar.

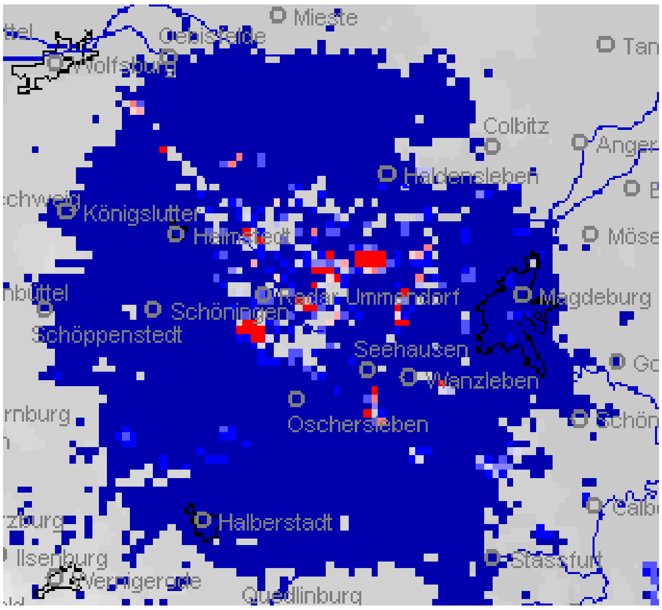

Figure 6.7: *Reflectivity data from the windmill farm near Ummendorf.*

8. DMI

Close by the Danish weather radar, Stevns, there is five windmills, 2.5 MW generators, which means the hub height is about 70 m above the surface, and the blades is about 40 m long. A map below, figure 8.1 shows the positions of the radar and the windmills. The radar is positioned where the bearing lines to the windmills meet.

Figure 8.1: *The radar's position is where the bearing lines from the windmills meet. The distance from the windmills is between 1.8 to 2.1 km and the bearing is from 315º and higher.*

The effect of windmill on the weather radars reflectivity image is among other effects seen on the figure 8.2 below.

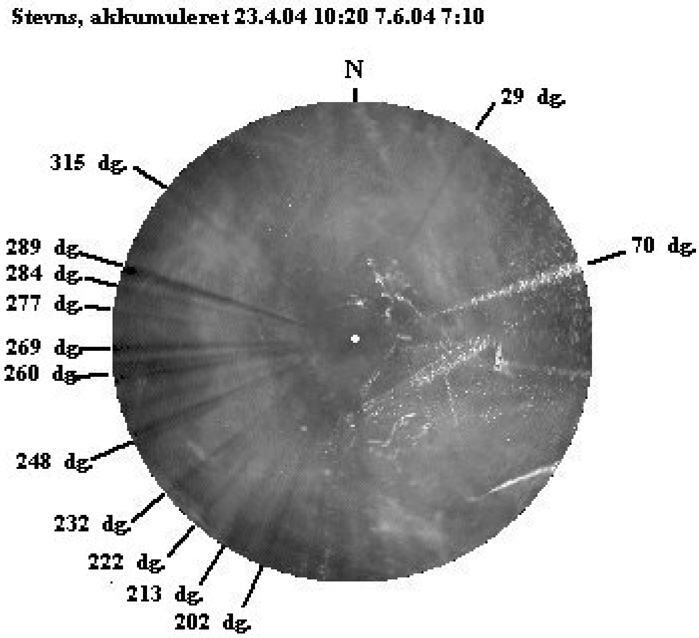

Figure 8.2: *Two weeks accumulated precipitation at the Stevns weather radar site, Denmark, showing the effects of radar beam blocking. The effects of three wind mills are seen at 315 dg. This image does not show the effect on Doppler measurements.*

This figure is produced by integrating the precipitation in one and a half month. The weather radar data is transformed from dBz to precipitation intensity (mm/hour) by using the Marchall-Palmer relation ($Z=a*R^b$, a=220 and b=1.6), and then performing an integration over time to produce an image showing the total precipitation in the period from 23.4.04 to 7.6.04. The image shows a lot of details, and blockage will show up as sectors of less intensity, eg. showing a loss of power in that sector.

On figure 8.3, the mean value of all bins in the rays ranging from azimuth 0º to 359º from figure 8.2, has been plotted. All the blockings has been marked with a vertical line. The blockings show up as a small dip in the value- On figure 8.4, the dip at 289º has been enlarged. One clearly sees a decrease in value from the level 15 mm of precipitation to 8 mm of precipitation in the time period, where the integration has been performed. This is nearly a halving of the signal! In table 1, all the blockings is listed.

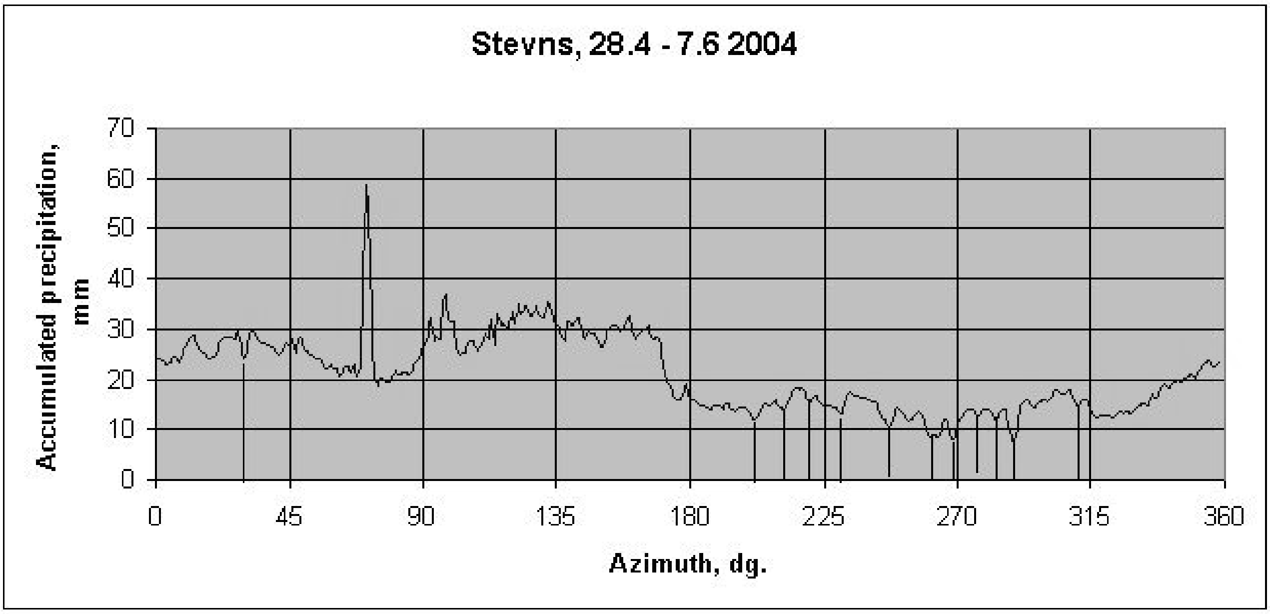

Figure 8.3: *Mean value of range bins (as total precipitation, mm) for each full degree of azimuth.*

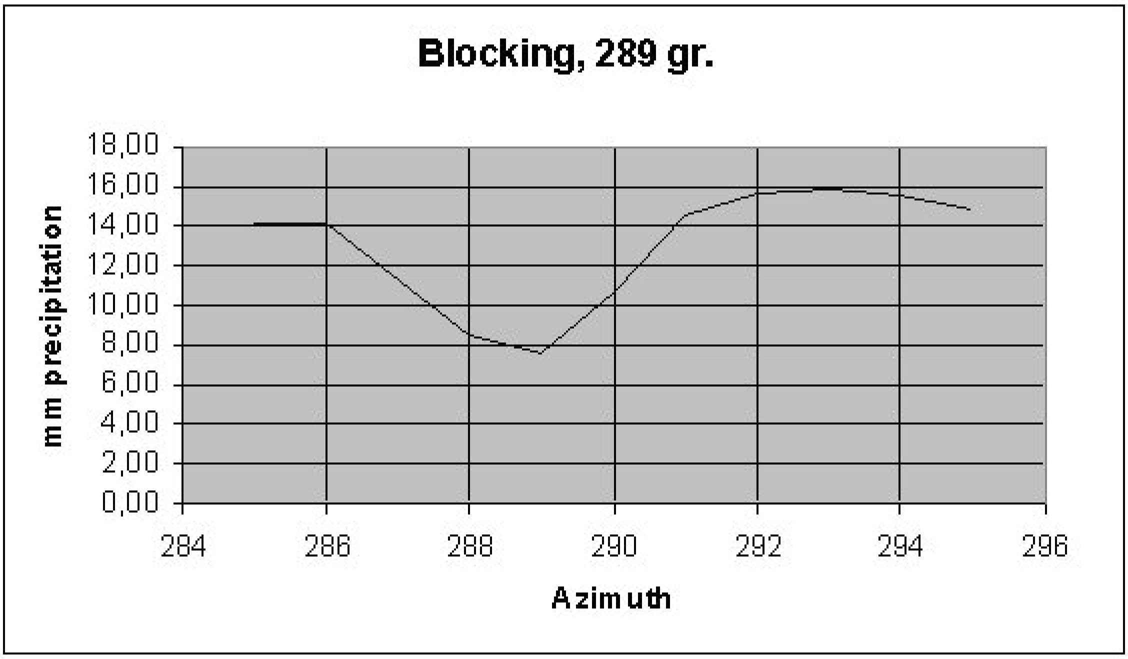

Figure 8.4: *A typical blocking expanded from figure 8.3 at 289 dg. The measured absolute precipitation in the period falls from a level of 15 mm to 8 mm.*

AZIMUT (GR.)	NIVEAU VALUE (MM)	MIN. VALUE (MM)
30	28,0	24,2
202	14,0	12,0
212	15,5	13,8
221	16,5	15,5
231	15,0	13,3
247	13,3	10,3
261	10,0	8,7
269	11,0	8,3
277	14,1	12,8
283	14,1	12,4
289	15,0	7,5
311	16,5	14,8

Table 1: *The measured differences in absolute precipitation, and hence the loss of energy.*

9. Recommendation

Figure 3.7 in chapter 3, demonstrates very clearly the devastating effect the wind mils farm have on the operational use of weather radars.

At a first glance, it confirms the huge dynamic of wind farms responses, due to blade movement. In the main beam, the equivalent RCS is about 23 dBm, which in radar context represents a huge energy. Also, the antennas side lobes show a huge signal. Relating this to Doppler measurements that are performed right above the radar sensitivity confirms the high potential threat of wind farms on Doppler products over very large area. Therefore the OPERA group has produced the statement below (OPERA WD_2006_13).

Statement of the OPERA group on the cohabitation between weather radars and wind turbines.

The OPERA group of EUMETNET:

- Considering the studies showing that the impact of wind turbines on weather radars are of three main types:
  - beam blocking
  - clutter
  - Doppler mode

- Considering the experience of cohabitation of European Meteorological Services, in particular Danish Meteorological Institute (DMI), Deutscher Wetterdienst (DWD), National Institute of Meteorology of Spain (INM), Royal Netherlands Meteorological Institute (KNMI), Météo-France and UK Metoffice,

- Considering that the most critical impact of wind turbines concerns the Doppler mode,

State:

1) That no wind turbine should be deployed at a range from radar antenna lower than:
  - 5 kilometers for C-band radars
  - 10 kilometers for S-band radars

2) That projects of wind parks should be submitted to an impact study when they concern ranges lower than :
  - 20 kilometers for C-band radars
  - 30 kilometers for S-band radars